



F. Mohaghegh *
Graduate Research Assistant

S. M. Hosseinalipour †
Associate Professor

M. M. Doustdar ‡
Asistane Professor

Parametric Study of Fuel Vapor Concentration Distribution Due to Vaporization of Fuel Droplets in Free Atmosphere

The growth of a two-phase cloud of a liquid fuel in a stagnant atmosphere is studied using computational fluid dynamic techniques. In order to predict the danger and hazard of such cloud in open atmosphere it is very important to determine the fuel concentration in the cloud, especially in the far field region from the fuel reservoir. The results show that with omission of droplets break up, the vaporization rate becomes very low due to large droplets and vapor cloud would be highly elongated. If the collision of droplets is neglected, vapor volume is higher. The results also show that when the height of device is increased, the cloud will have more symmetry. Any decrease in injection velocity leads to lower radial expansion of cloud. Reduction of injection time duration decreases the dangerous part of cloud slightly.

Keywords: droplet vaporization, vapor cloud expansion, concentration distribution.

1 Introduction

Nowadays, LPG (Liquefied Petroleum Gas) cylindrical gases are used widely in many houses and may cause danger to people because after dispersion of fuel from fuel vessel as a result of any crack, a two phase flow forms in the atmosphere in a way that the produced cloud contains liquid droplets, fuel vapor and air which can explode. One of the best ways of studying the hazard of the vapor cloud is the study of vapor cloud concentration in the open atmosphere.

The aim of this numerical analysis is to attain the effective parameters on a vapor cloud formed by dispersing droplets vaporization. The result of such study may have significant effects on hazard reduction of vapor cloud explosion.

Doustdar *et al.* [1] analyzed vaporization and dispersion of droplets injecting from a cylindrical vessel with KIVA software. KIVA is used to simulate flow and combustion of internal combustion engines, but they adapted it for external flows. The research concluded that if

* Engineering Research Institute, Tehran

† Corresponding Author, Mechanical Engineering Department and head of CAEC in Iran University of Science and Technology, Tehran, Email: Alipour@iust.ac.ir

‡ Head of Mechanical Engineering Department, Imam Hossein University, Tehran

the near field is known, the simulation of vapor cloud expansion could be done using the pressurized fuel from a series of injectors with small injection angles. Hosseinalipour *et al.* did a similar work with FLUENT [2].

The analysis of the far field regime is usually carried out for study of hazard and its management. Witcofski [3] studied hydrogen vapor cloud dispersion to obtain basic information regarding the physical phenomena governing the dispersion of flammable clouds formed as the result of spill of large quantities of liquid hydrogen. Instrumented towers located downwind of the spill site, gathered data of temperature, hydrogen concentration, and turbulence levels of the hydrogen vapor cloud expanding to downwind. Preliminary results of the experiments indicated that for rapid spills, thermal and momentum induced turbulences cause the cloud to disperse to safe concentration levels and becomes buoyant long before mixing due to normal atmospheric turbulence.

Vidal *et al.* [4] used SuperchemsTM software to calculate flammability of fuel under different initial conditions. They showed that a diluent like nitrogen or carbon dioxide can make a fuel-air system much safer due to reduction of flammability.

Science Applications International Corporation [5] discussed the hazard of vaporizing ammonia dispersing from vessels or pipes of Ammonia Refrigeration Facilities. It claimed that the dispersion of vapor cloud in rural areas with fewer ups and downs is much more hazardous than in urban areas.

Borysiewicz [6] developed an adaptive grid code to model urban dispersion using CFD method. LES has been used to model turbulence. The results were more efficient and had less time consuming calculations. For example the simulation of toxic plume in a wide area like a region in Manhattan with over 1000 buildings lasts only ten minutes.

The purpose of this study is to model the expanding fuel vapor cloud in the far field regime. A cylindrical vessel of liquid fuel with a distance from ground has been chosen. It is assumed that the vessel explodes and the fuel disperses into the air. After forming the vapor cloud by vaporizing droplets, the chemical reaction can be started by a spark or flame. The process can be divided in two different regimes, namely, near field and far field. In the near field, momentum exchange between droplets is stronger than the one between air and droplets. But the situation in far field regime is reversed. The main parameters in the near field regime such as temperature, pressure, velocity, mass concentration and also droplet size distribution affect the physics of the far field regime. The numerical analysis is done using FLUENT 6 software [7]. Effects of droplets break up, collision, height of vessel, distance from ground, injection velocity and injection time duration have been presented.

2 Physical and Mathematical Model

The flow is turbulent and Axisymmetric in a stagnant atmosphere. Calculation domain and the assumed boundary conditions are presented in Figure (1). Since the field is Axisymmetric, the cylindrical coordinates is used. The axis is coincided with the axis of cylinder vessel. Using axis has a bonus in analysis, because in this case two-dimensional analysis becomes available. Since in this paper, the effects of wind are neglected, the assumption is valid. The location of the far field regime starts from a 0.5m distance far from the axis. The device has 0.5m height and 0.5m distance from non-porous and smooth earth.

The used mesh for discretization of the calculation domain is presented in Figure (2-1). In order to study the independency of solution to the grid, a refined mesh as the one in Figure (2-2) was utilized.

2.1 Continuous Phase

The continuous phase modeling is based on finite volume analysis in which each transport equation is integrated over the control volume and discretized. The discretized transport equation contains the variable at the cell center as well as the unknown values in surrounding neighbor cells. Transport equations are relations of mass, momentum, energy, species and turbulence model in unsteady situation. In unsteady conditions all the equations are solved iteratively, for a given time-step, until the convergence criteria are met. The Upwind scheme was used to discrete the convection terms in the equations. This means that the face value is derived from quantities in the cell upstream, or “Upwind” relative to the direction of the normal velocity. Pressure and velocity coupling was forced using SIMPLE method. SIMPLE algorithm is used in subsonic flows and in supersonic flows when the flow has low compressibility [7]. The RNG turbulence model was used to calculate the turbulence parameters. The air is considered as an ideal gas with initial temperature equal to 310K. The ideal gas assumption is to consider the effects of flow compressibility.

Besides axis as the first boundary condition, the logarithmic law has been used for the wall boundary condition. For the two other boundary conditions the pressure has been fixed. The backflow viscosity ratio was fixed to 10 with a turbulent viscosity equal to 3 which are recommended by [2]. The convergence criterion was 10^{-8} in the residual of all equations.

2.2 Discrete Phase

The n-octane with initial mass of 15kg was considered as the fuel which was injected from twenty two parallel injectors within 5ms in the form of droplets with 3mm mean diameter and with Rosin-Rammler droplet distribution. The injection velocity was considered 250m/s.

• Forces Acting on Droplets

Because the density ratio of fuel to air was about 600, only drag and gravity forces were considered as the most important forces acting on the droplets [7]. The equation of motion for a single spherical droplet can be written as,

$$\frac{du_p}{dt} = g + \frac{3 \rho_g C_D}{4 \rho_l d_p} |u - u_p| (u - u_p) \quad (1)$$

In high relative velocities between droplet and air, gravitational forces are negligible in comparison with drag forces. So the main force affecting the droplet transport is the drag.

Due to the large distances between droplets, the effect of droplets on drag coefficient of each other is insignificant and in the estimation of the drag coefficient, each droplet can be considered separately [4].

Due to the fast motion of droplets, especially the bigger ones, they will deform and become non-spherical. The order of this effect depends on the size of the droplets. In order to consider the effect of droplets deformation, dynamic drag coefficient model for estimation of drag coefficient is used [7]. The model describes drag coefficient of each deformed droplet as a function of the drag coefficient of spherical ones:

$$C_d = C_{d,sphere} (1 + 2.632y) \quad (2)$$

The value of y is calculated using the following equation,

$$\frac{d^2y}{dt^2} = \frac{C_F \rho_g u_p^2}{C_b \rho_l r^2} - \frac{C_k \sigma}{\rho_l r^3} y - \frac{C_d \mu_l}{\rho_l r^2} \frac{dy}{dt} \quad (3)$$

• Droplet Break up Model

TAB or Taylor Analogy Break up model is used to model droplet break up [7]. This model is based upon Taylor's analogy between an oscillating and distorting droplet and a spring mass system. The analogy leads to

$$F - kx - d_p \frac{dx}{dt} = m \frac{d^2x}{dt^2} \quad (4)$$

in which

$$\frac{F}{m} = C_F \frac{\rho_g (u - u_p)^2}{\rho_l r}, \quad \frac{k}{m} = C_k \frac{\sigma}{\rho_l r^3} \quad \text{and} \quad \frac{d_p}{m} = C_d \frac{\mu_l}{\rho_l r^2} \quad (5)$$

A droplet breaks up, if the distortion grows to a critical ratio of the droplet radius:

$$x > C_b r \quad (6)$$

The size of the child droplets is determined by equating the energy of the parent droplet to the combined energy of the child droplets. The energy of the parent droplet is

$$E_{\text{parent}} = 4\pi r^2 \sigma + K \frac{\pi}{5} \rho_l r^5 \left[\left(\frac{dy}{dt} \right)^2 + \omega^2 y^2 \right] \quad (7)$$

ω is the droplet collision frequency obtained from equation

$$\omega = \sqrt{\frac{C_k \sigma}{\rho_l r^3} - \left(\frac{2\rho_l r^2}{C_d \mu_l} \right)} \quad (8)$$

The energy of the child droplets is equal to

$$E_{\text{child}} = 4\pi r^2 \sigma \frac{r}{r_{32}} + \frac{\pi}{6} \rho_l r^5 \left(\frac{dy}{dt} \right)^2 \quad (9)$$

The child droplets will have a velocity normal to the parent droplet velocity given by

$$v_{\text{normal}} = C_v C_b r \frac{dy}{dt} \quad (10)$$

• Droplet Collision

O'Rourke's algorithm is used to model the collision of droplets [7]. The model assumes that the probability distribution of the number of collisions follows a Poisson distribution:

$$P(n) = e^{-\bar{n}} \frac{\bar{n}^n}{n!} \quad (11)$$

The probability of coalescence is related to the offset of the larger droplet center and the trajectory of the smaller droplet. If the droplets collide head-on, the outcome of collision tends to be coalescence. If the collision is more oblique, the collision results in bouncing of droplets. Thus, a critical offset b_{crit} is considered to study the collision outcome of two droplets with radius r_1 and r_2 :

$$b_{\text{crit}} = (r_1 + r_2) \sqrt{\min\left(1.0, \frac{2.4f}{We}\right)} \quad (12)$$

where f is a function of r_1/r_2 defined as

$$f = \left(\frac{r_1}{r_2}\right)^3 - 2.4\left(\frac{r_1}{r_2}\right)^2 + 2.7\left(\frac{r_1}{r_2}\right) \quad (13)$$

and We is the Weber number defined as

$$We = \frac{\rho U_{\text{rel}}^2 \bar{D}}{\sigma} \quad (14)$$

Equation (12) can be used in a way that if the offset is less than b_{crit} , the collision is coalescence. The properties of the coalesced droplets are found from the basic conservation laws. Otherwise, when the offset is greater than b_{crit} , the droplets exchange momentum and kinetic energy and the new velocities are calculated based on conservation of momentum and kinetic energy.

• Droplet Vaporization Model

Droplet vaporization rate is calculated from

$$\dot{m}_1 = k_c A_p (C_{i,s} - C_{i,\infty}) \quad (15)$$

where \dot{m}_1 is mass transfer due to vaporization and k_c is binary diffusivity coefficient which depends on material. In this study the coefficient is $2.9 \times 10^{-5} \text{ m}^2/\text{s}$ for n-octane and air binary diffusivity. A_p stands for surface area of droplet, $C_{i,s}$ and $C_{i,\infty}$ are concentration of vapor in droplet surface and bulk of continuous phase, respectively.

3 Results

To investigate the maximum hazards, a range of mass fraction for fuel vapor in the air is considered in which the reaction leads to detonation that is much more devastating than deflagration. This range is between 0.04 and 0.24 for n-Octane [1]. The aim is to study the maximum volume of the detonable part. Table (1) presents different cases which were studied in this work.

Table 1 Different cases in present research

	<i>Droplet break up</i>	<i>Droplet collision</i>	<i>Low height from earth</i>	<i>Low injection velocity</i>	<i>Low injection time duration</i>
1	Yes	Yes	Yes	No	No
2	No	Yes	Yes	No	No
3	Yes	No	Yes	No	No
4	Yes	Yes	No	No	No
5	Yes	Yes	Yes	Yes	No
6	Yes	Yes	Yes	No	Yes

Figure (3) presents the vapor cloud expansion for the first case. It can be inferred from the figure the effects on the following items:

- **Vapor cloud expansion**

Rate of vapor cloud expansion is lower than initial droplet velocity. This shows the prevailing effect of drag force as in Figure (3). Cloud expansion velocity (at the order of 20m/s) is much lower than injection velocity of droplets i.e., 250m/s. During the droplet dispersion, droplet size distribution is very different due to droplet break up and droplet field is full of small and large droplets which are smaller than the initial droplet size. Velocity of small droplets reduces more rapidly than larger ones, because

$$\left. \begin{array}{l} F \propto d^2 \\ m \propto d^3 \end{array} \right\} \Rightarrow a = \frac{F}{m} \propto \frac{1}{d} \quad (16)$$

Because of droplet break up phenomenon, a very large number of droplets are produced from initial large droplets which enhance the effect of drag force in the droplet motion field.

- **Cloud expansion in direction normal to injection direction**

Due to shear stresses acting on the interface of the vapor cloud moving in a stagnant air and also turbulence velocity fluctuations, the expansion of the vapor cloud occurs in the normal direction to the injection. Cloud expansion reduces with time in vertical direction due to shear stress and turbulence dissipation as a result of velocity reduction.

- **Ground effect**

With forward expansion of vapor cloud, effect of ground becomes more pronounced. At initial stages of the cloud formation, the shape of the cloud is rather Axisymmetric. This symmetry diminishes as the cloud expansion continues and the effect of ground enhances.

- **The most hazardous instant**

Due to velocity reduction of droplet, vaporization rate reduces. With elapse of time, the droplets velocity reduces to an amount that droplet vaporization cannot compensate the expansion of detonable part of cloud. Thus the vapor concentration drops to an amount lower than detonable concentration. The instant of maximum detonable part of cloud is the most hazardous moment for a spark to start the detonation, because the spark has more chance to lead to detonation.

Figure (4) shows variation of detonable vapor cloud. Based on this figure, in the instant of 100ms the vapor cloud has the maximum volume of detonable part.

- **The most hazardous position**

The detonable part of cloud which is the most hazardous position grows at first stages and proceeds at positive radial direction. With reaching the ground and lying into the boundary layer, the height of region lowers, but it expands towards the ground.

In order to study the results of other cases, instant of 100ms in which the detonable part of volume has its higher value has been chosen to compare the results. The comparison results are as following:

3.1 Droplet break up effect

To investigate the effect of droplets break up, the second simulation was carried out neglecting this effect. The results are presented in Figure (5). The figure shows that if the larger droplets do not break up to smaller ones, the cloud shape will be narrow. As mentioned before, larger droplets are less affected by fluctuating velocity components than the smaller ones and they can continue their path better. Since the turbulence diffusivity has low impact on large droplets, the height of cloud would be less than the first case. In this case the cloud expansion rate is very high due to higher droplet speed and less drag effect on large droplets.

In the second case, maximum vapor cloud concentration does not reach any appropriate concentration for detonation and the cloud concentration is about 1/500 of the first case. The reason is the increase of droplet-air interface area with break up. Break up produces more droplets with sizes in the order of microns. Therefore, there will be large surface area for heat and mass transfer between the droplets and the surrounding air.

3.2 Droplet collision

In the third case, collision of droplets has been deleted and just the break up has been considered. The result is presented in Figure (6). In this case, the average droplet size is less than the first case. As it is shown the following results can be concluded in the comparison with the results for case 1,

- Radial extension of cloud is lower (about 5%)
- Overall cloud size is lower (about 5%)
- Droplets have more vaporization rate (about 15% more detonable part volume)

When the droplets are smaller as a result of omitting the collision, the effect of the drag force on them increases and they will have less velocity. So the shear flow is weaker and the radial extension of cloud becomes lower. Overall vapor cloud size also decreases as a result of less droplets velocity. More interface area for heat and mass transfer, causes the droplets vaporization become higher.

3.3 Distance from earth

In order to investigate the effect of ground on the vapor cloud expansion more precisely, the distance of device from ground has risen to 1m for the fourth case. Figure (7) displays the results for this case. It is obvious that the expansion rate of the cloud in vertical direction becomes more pronounced with respect to the first case at about 15%. In this case, larger distance from earth causes the vapor to sense the earth later and progress more. With a similar reason, the detonable part of the cloud has more symmetry. This region is farther from injectors and the detonable part of cloud is less due to stronger cloud expansion.

3.4 Injection velocity

The fifth case is similar to the first one, but with lower injection velocity, namely 150m/s. As shown in Figure (8), the cloud forward expansion is lower, the height of cloud is shorter and the detonable part do not detach from the axis. Lower injection velocity results in less droplet penetration in the stagnant air and therefore, the cloud volume would become less.

3.5 Injection time duration

For the last case, injection time duration has been reduced from 5ms to 1ms. The results are shown in Figure (9). The cloud in this case has less volume than the first case and the detonable part of cloud shows a clear reduction in volume.

The reduction in injection time duration causes the closer droplets and lower vaporization rates.

4 Validation of the Results

To investigate the independency of solution to grid types, modified grid of Fig (2-2) was used. The result of mass fraction of n-octane over a horizontal line in a 0.75cm distant from the ground is presented in Figure (10). It is evident that the results are almost identical and the overall differences are less than 10%.

In order to have a comparison with other sources, data of Doustdar *et al.* [1] in the instant of 100ms has been chosen and presented in Figure (11). All the conditions are the same as the first case. It is evident that although the overall shape of the cloud is the same for both studies, the concentration of fuel vapor is higher in [1]. The main reason is the difference between droplet vaporization model in FLUENT and KIVA CFD software which was used by Doustdar *et al.* The vaporization model of FLUENT is Equation (15) but the vaporization model of KIVA is based on the equation:

$$\dot{m}_1 = k_c A_p \ln \left(1 + \frac{C_{i,s} - C_{i,\infty}}{1 - C_{i,s}} \right) \quad (17)$$

When the vaporization rate is low, $C_{i,s}$ approaches zero and Eqs. (15) and (17) become almost the same. However, when the vaporization rate increases, the difference of the results grows. The difference of the two models for n-octane is 13% in this case.

The other reason for differences between two studies is the difference of the used fuel. Doustdar *et al.* used gasoline instead of n-octane in their work. Although both fuels are rather similar, gasoline is a fuel mixed of hydrocarbons many of them are more volatile. Rapid vaporization of these components and late evaporation of the other one changes the vaporization pattern slightly and causes more difference.

5 Conclusion

The cloud expansion is much lower than the initial injection velocity. It expands in vertical direction with symmetric shape at first stages, but the symmetry destroys due to ground effect. The detonable part of cloud grows at first, but with initial velocity reduction and thus decrease of vaporization rate, the volume shrinks. The volume at first proceeds at positive radial direction and with reaching the ground and lying into the boundary layer, the height of region lowers, but it expands in the opposite radial direction.

Vaporization rate at first has its maximum level during which droplets relative velocity has its highest level. With reduction of droplet velocity, the vaporization rate diminishes. Neglecting the droplets break up leads to incorrect results. In this case the vaporization rate is very low due to presence of large droplets. When the break up occurs, the interaction surface of droplets increases drastically which causes an increase in mass and energy transfer rates due to higher surface area

of droplets. When the break up is not modeled, effect of the turbulence fluctuations will be very low and thus the vapor cloud will be very elongated. In the case with neglected droplets collision model, vapor volume becomes larger.

With increase of device height, the effect of ground will be sensed later; therefore cloud will have more symmetry. Decrease of injection velocity leads to lower radial expansion of cloud and the detonable part of cloud approaches more towards the axis. The detonable part of cloud is slightly larger in this case. With reduction of injection time duration, the detonable part of cloud decrease slightly.

Proof Read

References

- [1] Doustdar M., Hosseinalipour, M., and Mazaheri K., "Numerical Study of Two-phase Unconfined Fuel Air Cloud Characteristics to Consider its Detonability", Proceeding of the 10th annual conference of the CFD Society of Canada, Canada, Windsor, pp. 204-210, (2002).
- [2] Hosseinalipour, S. M., and Mohaghegh, F. M., "Simulation of Dispersion and Vaporization of Dilute Droplet Flow", Iranian eighth conference of fluid dynamics, Iran -Tabriz, September, (2003).
- [3] Witcofski R. D., "Dispersion of Flammable Vapor Clouds Resulting from Large Spills of Liquid Hydrogen", NASA Technical Memorandum 83131, Atlanta GA, USA, MAY 1981.
- [4] Vidal, M., Wong, W., Mannan, M. S., and Rogers, W. J., "Evaluation of Lower Flammable Limits of Fuel-air-diluent Mixtures", Mary Kay O'Connor Process Safety Center, Artie McFerrin Department of Chemical Engineering Texas A&M University, College Station, Texas 77843-3122, USA.
- [5] Science Applications International Corporation, "Model Risk Management Program and Plan for Ammonia Refrigeration", *Science Applications International Corporation*, Environmental Protection Agency (EPA), May 1996, Reston, VA.
- [6] Borysiewicz, M.J., "Models and Techniques for Health and Environmental Hazards Assessment and Management", MANHAZ MONOGRAPH, IEA, Poland, Swierk, Summer Workshop (2005).
- [7] ANSYS.Inc company, "FLUENT 6 User's Guide Manual", Santa Clara, CA U.S.A, 2006.

Nomenclature

A_p	: Surface area of droplet
b_{crit}	: Critical offset of collision
C_b	: Constant equal to 5
C_D	: Drag coefficient of droplet
$C_{D,sphere}$: Drag coefficient of sphere
$C_{i,s}$: Drag coefficient of sphere
$C_{i,\infty}$: Vapor concentration in droplet surface bulk of continuous phase
C_F	: Constant equal to 1/3
C_k	: Constant equal to 8
C_v	: A constant of order one
\bar{D}	: Arithmetic mean diameter of two droplets
d, d_p	: Droplet/Particle diameter
E	: Kinetic energy of a droplet
F	: Droplet acting force
g	: Gravitational force
K	: The ratio of the total energy in distortion to the total energy
k_c	: Binary diffusivity coefficient
m	: Droplet mass
\dot{m}_1	: Mass transfer due to vaporization
n	: Number of collisions among droplets
$P(n)$: Poisson distribution
r	: Droplet radius
r_{32}	: Sauter mean radius of the droplet size distribution
t	: Time
We	: Weber number
u	: Velocity of continuous phase
u_p	: Velocity of discrete phase
U_{rel}	: Relative velocity between two droplets
v_{normal}	: Velocity normal to the parent droplet velocity
x	: Droplet distortion
y	: Normalized droplet distortion
μ_1	: Viscosity of the specified droplet
ρ_g	: Density of continuous phase
ρ_l	: Density of discrete phase
σ	: Surface tension of droplet
ω	: Droplet collision frequency

Figures

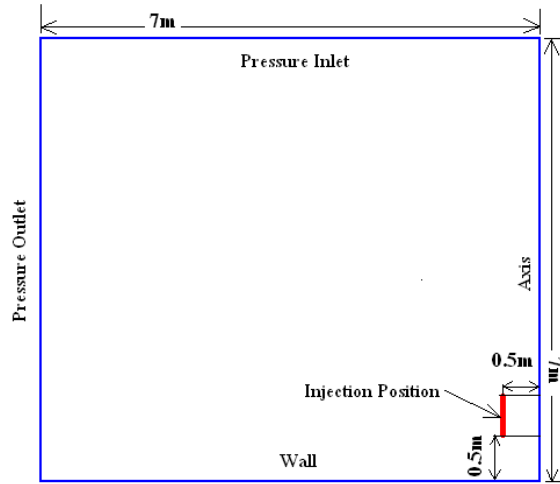


Figure 1 Calculation domain boundary condition

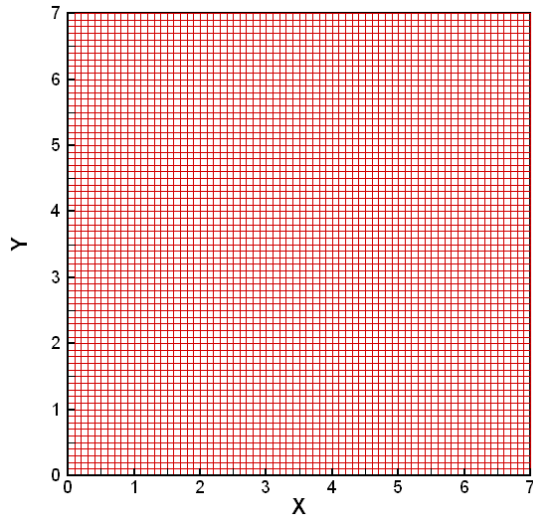


Figure 2-1 Mesh used for numerical solution

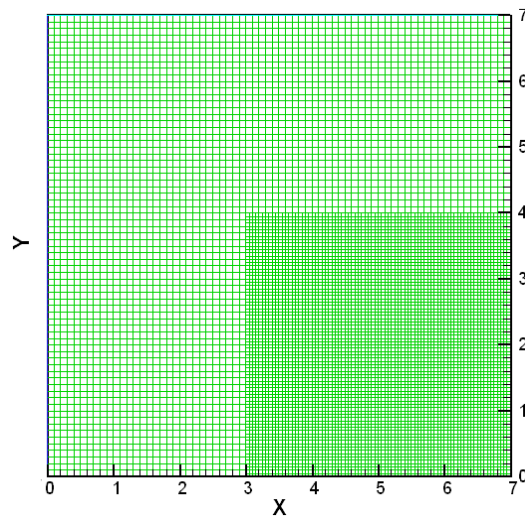


Figure 2-2 Adapted Mesh for grid independency proof

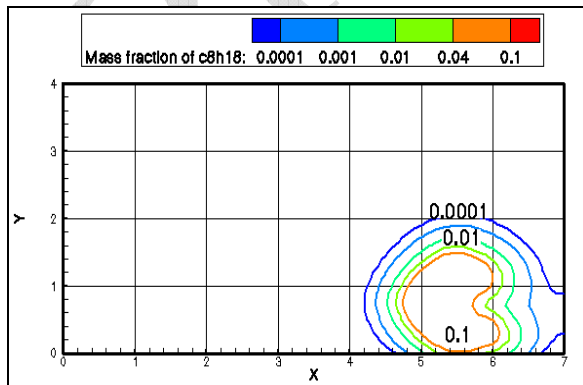


Figure 3-1 Mass Concentration at 20ms (Case 1)

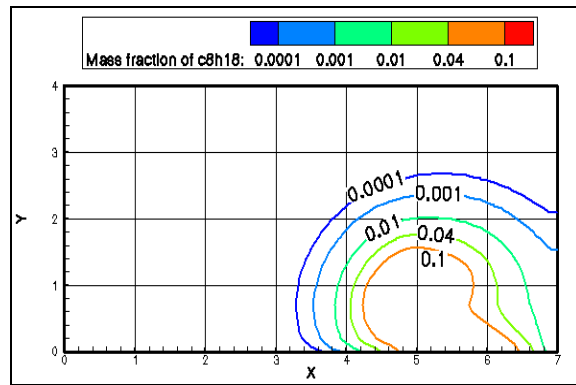


Figure 3-2 Mass Concentration at 50ms (Case 1)

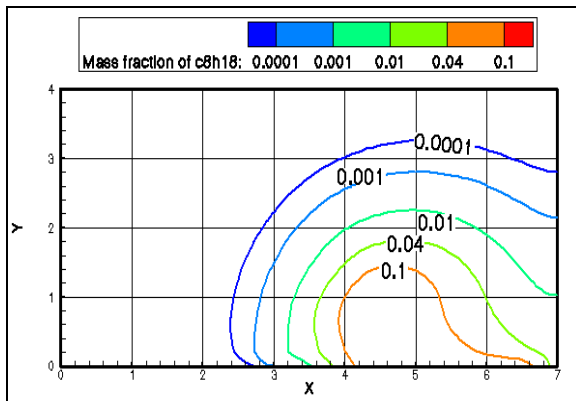


Figure 3-3 Mass Concentration at 100ms (Case 1)

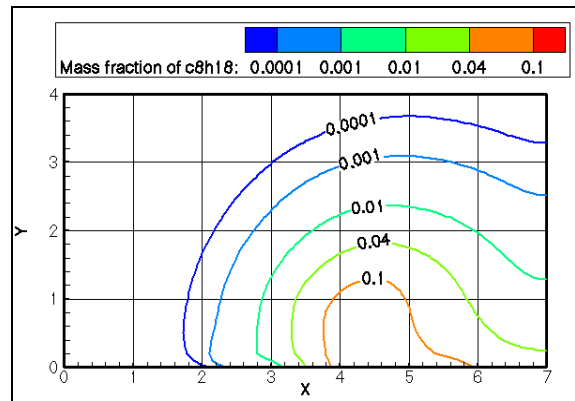


Figure 3-4 Mass Concentration at 150ms (Case 1)

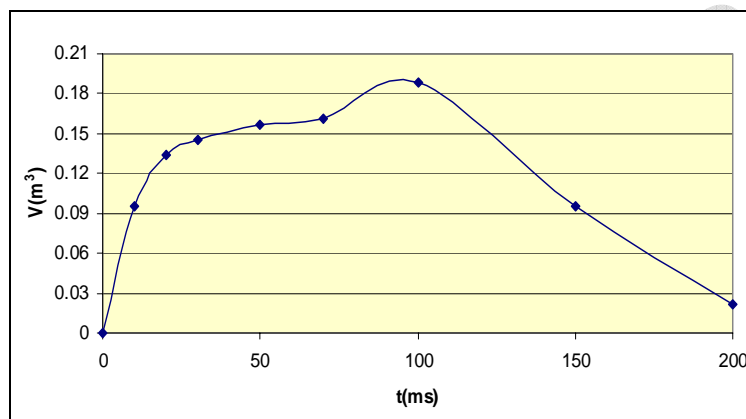


Figure 4 Detonable part of vapor cloud volume (Case 1)

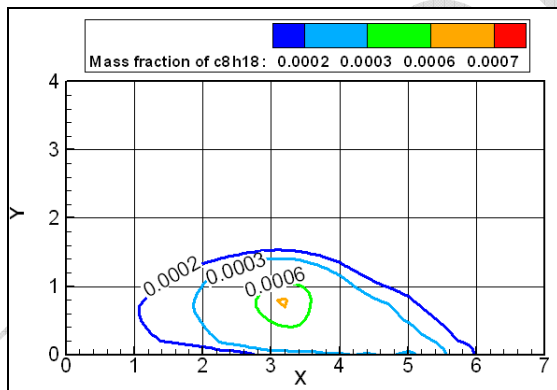


Figure 5 Mass Concentration without break up modeling (Case 2)

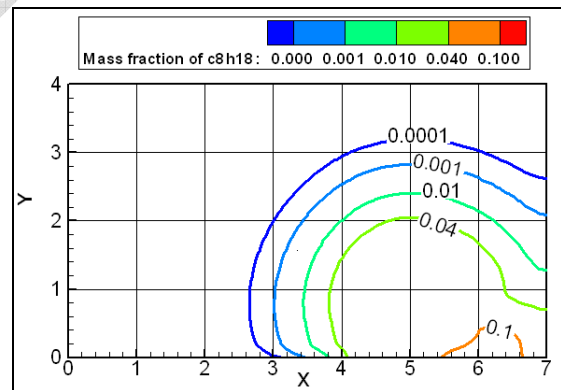


Figure 6 Mass Concentration without collision modeling (Case 3)

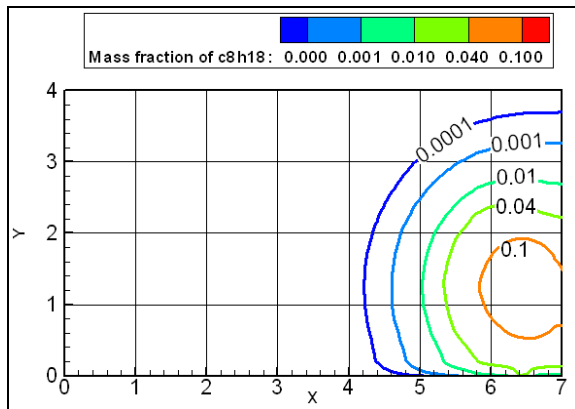


Figure 7 Mass Concentration at high height (Case 4)

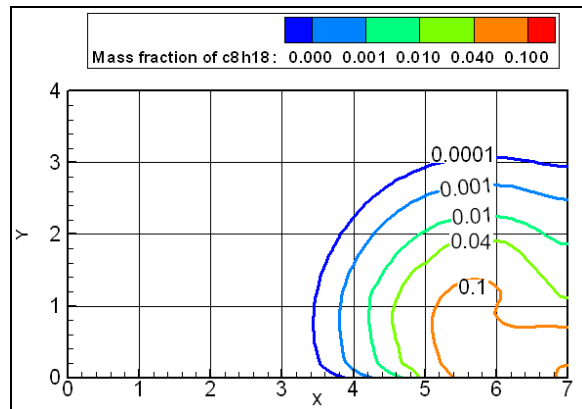


Figure 8 Mass Concentration at low injection velocity (Case 5)

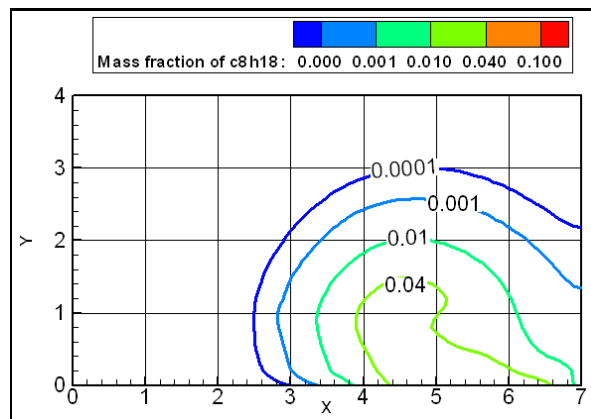


Figure 9 Mass Concentration at low time duration (Case 6)

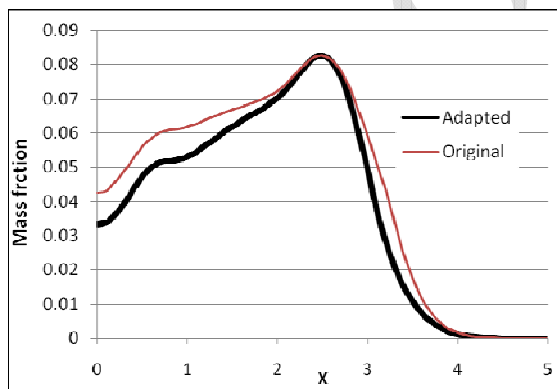


Figure 10 Variation of Mass Concentration with mesh adaptation

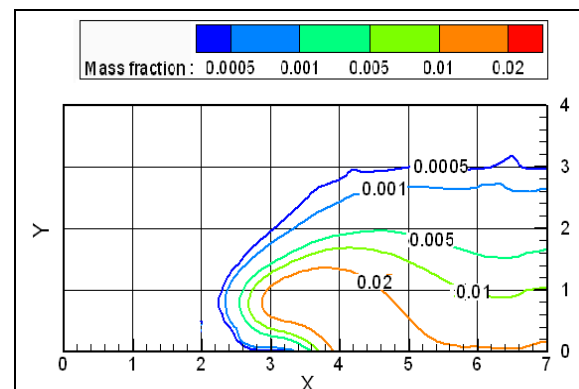


Figure 11 Comparison of results with [1]

Proof Read